Availability of artificial neural network for estimation of consolidation properties of Holocene clays in Osaka Bay

Kazuhiro Oda[1#], *Shoko* Yamamoto[2], Masahiro Kondo[2], and Toru Inui[3]

[1]*Osaka Sango University, Department of Urban Creation, 3-1-1 Nakagaito Daito Osaka, Japan*
[2] *JR West Japan Consultants Company, Civil Engineering Design, 5-4-20 Nishinakajima, Yodogawa, Osaka, Japan*
[3]*Osaka University, Department of Civil Engineering, 2-1 Yamada-oka Suita Osaka, Japan*
[#]*Corresponding author: oda@ce.osaka-sandai.ac.jp*

ABSTRACT

In this study, artificial neural network, a popular machine learning technique, was used to estimate the consolidation properties of points where no soil investigations have been conducted. The Holocene clay layer at the construction site of Kobe Airport, a large-scale man-made island in Osaka Bay, was targeted to estimate the consolidation properties. The performance of an estimation model built with artificial neural network depends on the datasets used during the training phase. Therefore, the average of multiple estimation results can be used. Numerical simulations using the estimated consolidation properties can accurately reproduce the settlement behavior owing to reclamation during the construction of Kobe Airport. Artificial neural network can easily and objectively estimate the consolidation characteristics of any point based on the existing soil investigation results.

Keywords: ISC7; artificial neural network; consolidation; numerical analysis; clay.

1. General instructions

Generally, boring investigations are conducted specifically for construction projects to understand the geotechnical characteristics of construction sites. Once the design of the structures built at the construction site is complete, soil investigations are rarely used thereafter. In Japan, there has been a shift away from this approach, with several movements aimed at accumulating and utilizing geotechnical information obtained from soil investigations. Particularly in the Kansai region, which is the second largest region in Japan, the accumulation, management, research, and engineering reuse of geotechnical information has been promoted since the mid-1980s. In recent years, accumulated geotechnical information has been applied to building information modelling (BIM).

One of the most important applications of existing geotechnical information is the estimation of geotechnical information at points where no soil investigations have been conducted. Geotechnical information was estimated subjectively by geotechnical engineers based on their experience.

In recent years, artificial neural network has been adopted in various fields, and its applications have expanded. Artificial neural network has the potential to replace human judgments based on experience and intuition. Therefore, if artificial neural network can replace previous subjective estimations of geotechnical information, it can be interpreted objectively. Consequently, the estimated geotechnical information could be interpreted both statistically and probabilistically.

In this study, a method was developed to build a model to estimate the consolidation properties of arbitrary points based on the results of existing boring investigations of Holocene clay layer using artificial neural network. A numerical simulation of the construction process of Kobe Airport was conducted using the estimated consolidation properties. The simulation results were compared with actual measurements to verify the validity of the proposed method.

2. Artificial neural network

Artificial neural network is a representative form of artificial intelligence that emulates the neural circuits in the human brain. Figure 1 schematically illustrates the architecture of the artificial neural network used in this study. The architecture consists of an input layer, output layer, and hidden layers that connect the input and output layers. The explanatory variables were provided to the network through the input layer. Following the computational processing within artificial neural network, the outcome is delivered through the output layer.

In Figure 1, the four lines from each solid blue circle are connected to the four hollow circles. The hollow circles are representative of neurons. These lines transmit signals from the first to the next layer. The signal transmitted in the neuron is mathematically manipulated using the following formula:

$$\theta = \sum_{i=1}^{n} w^k{}_i x^k{}_i + \beta^k{}_j \tag{1}$$

$$x^{k+1}{}_j = f(\theta) \tag{2}$$

where k is the level of the hidden layer; n is the number of neurons at kth level of the hidden layer; x^k_i is the signal transmitted from the ith neuron at the k-1th level of the hidden layer to the jth neuron at the kth level of the hidden layer; w^k_i is the weight of the ith signal at the kth level; and β^k is the bias at the kth level. The signal transmitted from the jth neuron in the kth level to the neurons in the $k+1$th level of the hidden layer is calculated by an activation function f. Typically. The rectified linear unit (ReLU) function is typically used for artificial neural network. Figure 1(b) shows the ReLU function. The ReLU function is given by:

$$x^{k+1}_j = 0 \quad \theta \le 0 \tag{3}$$

$$x^{k+1}_j = \theta \quad \theta > 0 \tag{4}$$

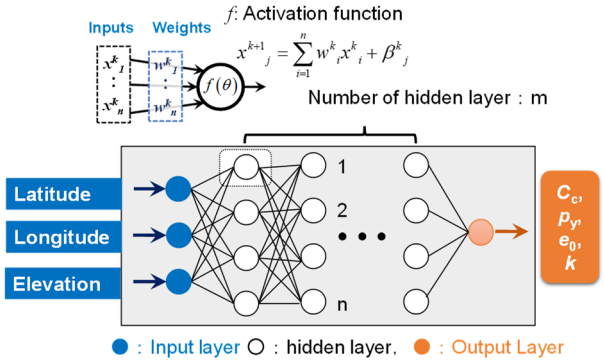

(a) Schematic view of artificial neural network

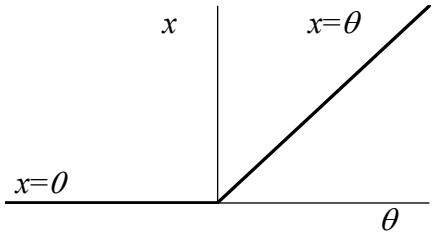

(b) Activation function (ReLU)

Figure 1. Schematic illustration of the network and activation function used for artificial neural network.

The hidden layer forcibly associates the explanatory variables from the input layer with the target variables of the output layer, even if there is no theoretical relationship. Moreover, by complicating the hidden layers, that is increasing the number of neurons and making the hidden layers more multilayered, the expressiveness of the target variables in the output layer is enhanced. However, complicating the hidden layers results in a number of unknown parameters w_i and β, therefore, a large number of datasets are required to build an appropriate neural network.

Artificial neural network does not innately possess intelligence. As humans develop through continuous learning from birth, training to optimize the unknown parameter w_i β is essential. This training phase utilizes a dataset of predefined explanatory and actual target variables, iteratively adjusts w_i and β minimizes the discrepancy between the estimated and actual target variables using artificial intelligence techniques. The purpose of this study is to develop a model for estimating the spatial distribution of consolidation properties. Consequently, geographic coordinates, Latitude, Longitude, and Depth were adopted as explanatory variables and consolidation properties, specifically, the void ratio, compression index, consolidation yield pressure, and coefficient of permeability, were adopted as target variables for estimation.

Figure 2 illustrates the conventional framework for developing an artificial intelligence system, which comprises two primary phases: training and testing. During the training phase, the model parameters w^k_i and β^k within the activation function of each neuron, as shown in Figure 1, were calibrated using 70% of the available sample data. This calibration aims to reduce the discrepancy between the model's estimations and the actual target variables. Consequently, an estimation model is built and fine-tuned to accurately estimate the outcomes represented by the training dataset. This necessitates the verification of the model's efficacy in estimating the consolidation properties at any given geographical coordinate. Subsequently, the testing phase involved evaluating the model's predictive accuracy using the remaining 30% of the sample data, which were withheld from the training phase, to ensure the model's robustness and reliability.

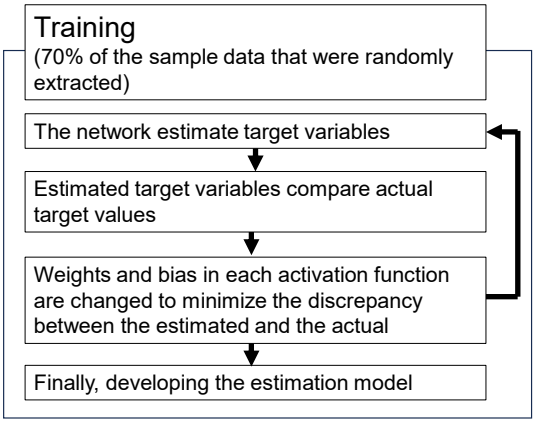

(a) Artificial neural network training phase

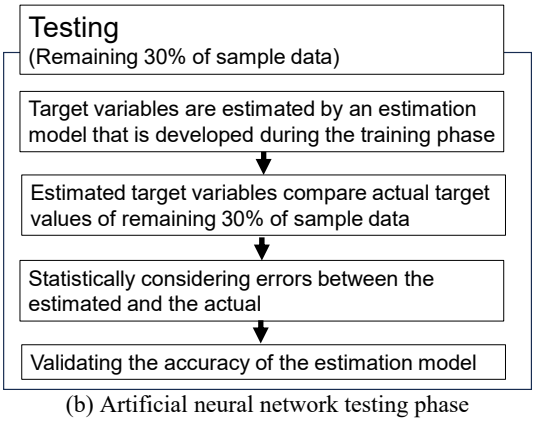

(b) Artificial neural network testing phase

Figure 2. Conventional framework for developing artificial neural network.

3. Kobe Airport

Figure 3 shows the location of Kobe Airport, which was constructed on a manmade island in the northern section of Osaka Bay. Therefore, there are two large-

scale airports in Osaka Bay, Kansai International Airport and Kobe Airport, which are man-made offshore islands.

Figure 3. Location of the Kobe Airport

Figure 4 shows an example of the soil profile below the seabed at Kobe Airport. The soil profile includes a Holocene clay layer identified as Ma 13, which is characterized by its soft skeleton and high compressibility. Beneath this layer, a sequence of Pleistocene clay layers was found, labeled Ma 12, Ma 11, Ma 10, and Ma 9. These layers signify a geological transition to older and denser sediments. Additionally, the profile features Pleistocene layers designated Ds1, Ds2, Ds3, Ds4, Ds5, Ds8, Ds9, and Ds10, which predominantly consist of coarse-grained soils, indicating different compositions and structural characteristics compared to the overlying Holocene clay.

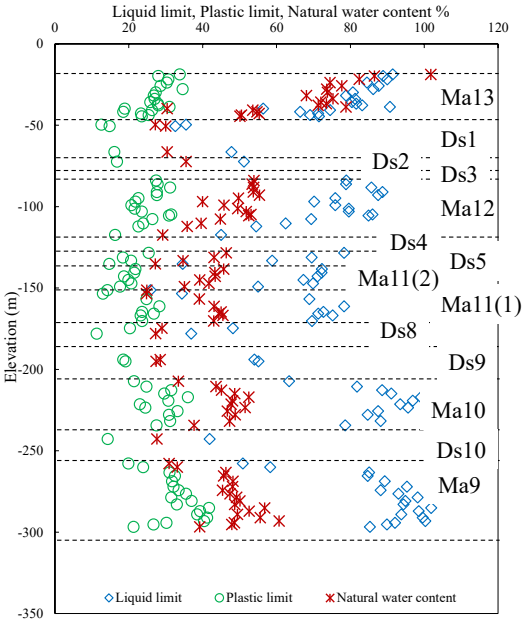

Figure 4. Example of soil profile below Seabed at Kobe Airport

Figure 5 shows the locations selected for the boring investigations, which are essential for the development of the estimation model and the locations for the determination of consolidation properties. Fifty boring investigations, represented by the solid blue circles, contributed to the construction of the estimation model. Numerous investigations have been conducted in revetment areas of Kobe Airport Island. On the other hand, only a limited number of boring investigations have been carried out in runways, passenger terminals, and control towers, which are important airport facilities. KC-1, represented by a red solid circle, is the point at which the estimation was performed. At this point, field measurements of settlement were performed to maintain the runway.

The results of the oedometer tests in these boring investigations were sourced from the Kansai Geoinformatics Database (Mimura et al., 2014), which currently contains approximately 90000 boring investigations conducted in the Kansai and Shikoku regions. Table 1 lists the sizes of the datasets used in this study. The dataset size utilized for building the estimation model for the permeability coefficient is approximately 8.5 times larger than that for other parameters. The coefficient of permeability was derived at each loading increment in the oedometer tests specifically for the development of the estimation model for the coefficient of permeability.

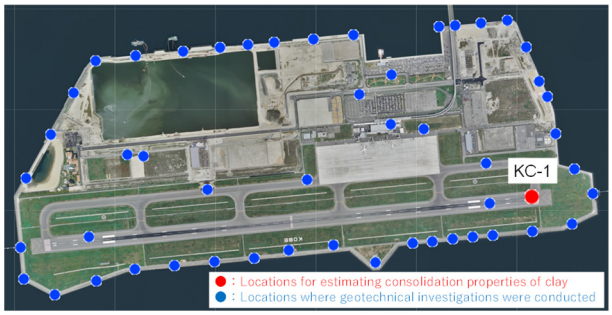

Figure 5. Locations for geotechnical investigations and estimation of consolidation properties for developing the estimation model.

Table 1. Number of dataset size

Void ratio	657
Consolidation yield stress	657
Compression index	657
Coefficient of permeability	5566

4. Performance of estimation model

The goal of building the estimation model was to accurately emulate the datasets used in the training phase (Figure 2). Therefore, the performance of the estimation model depends on the dataset used for training. This indicates that changing the dataset affects the performance of the estimation model. To investigate the impact of the training datasets on the performance of the estimation model, a series of parametric studies was conducted.

Table 2 presents the architectures of the estimation models used in this study6. For the parametric study, 100 datasets were randomly selected from the sample and used to build an equal number of estimation models during the training phase. The performance of each model is evaluated during the testing phase. (Oda et al. 2023).

Table 2. Architecture of artificial neural network in parametric study

Case	Neurons	Hidden layers
02N010	10	2
02N020	20	2
02N040	40	2
04N040	40	4

Figures 6–8 show the distributions of the mean absolute errors of the void ratio, compression index, and consolidation yield pressure during the training and

testing phases, respectively. Figure 9 shows the mean absolute error distribution of the logarithm of the coefficient of permeability during these phases. In the parametric study, the number of neurons and hidden layers in the model were varied to investigate their impact on the performance of the estimation model. It was observed that as the number of neurons and hidden layers increased, the architecture of the estimation model became more complex, resulting in a gradual decrease in the mean absolute error and an improvement in the model accuracy. However, the variation in the mean absolute error still remained unchanged, indicating that the estimated consolidation properties varied. To mitigate the effect of this variation, subsequent analyses adopted the mean value of each estimation result as the representative value of the estimation. Furthermore, 04N040 was adopted as the optimal artificial neural network architecture.

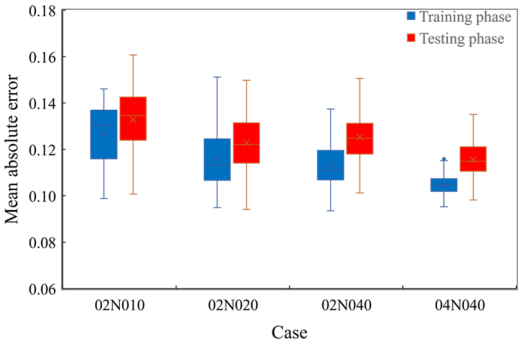

Figure 6. Distribution of mean absolute error for training and testing phases relative to void ratio

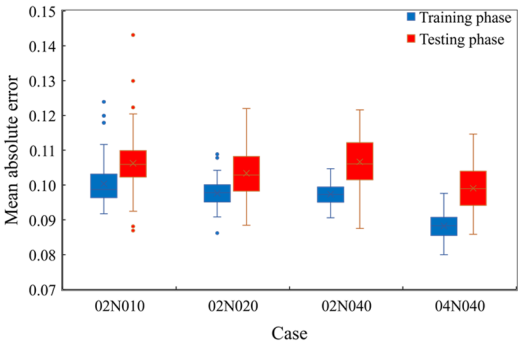

Figure 7. Distribution of mean absolute error for training and testing phases relative to compression index

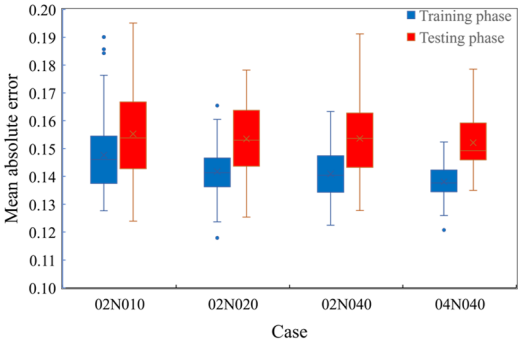

Figure 8. Distribution of mean absolute error for training and testing phases relative to consolidation yield pressure

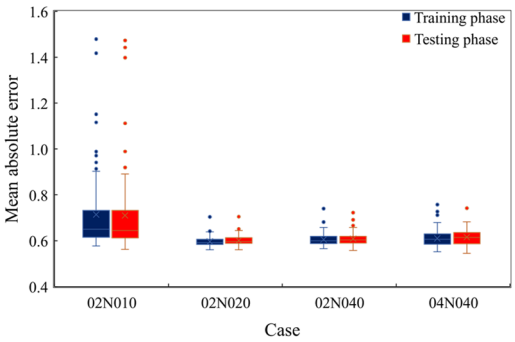

Figure 9. Distribution of mean absolute error for training and testing phases relative to the coefficient of permeability

5. Estimation of consolidation properties using artificial neural network

Figure 10 shows the estimated void-ratio distribution with depth at KC-1. The hollow circles represent the void ratios from the soil investigations conducted in the vicinity of KC-1. The void ratio monotonically decreases with depth, ranging from approximately 3.0 to 1.5 (Hasegawa et al. 2007a).

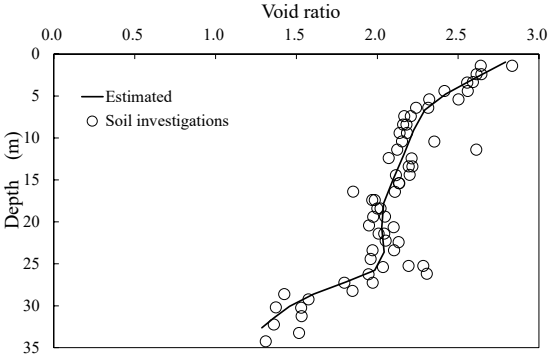

Figure 10. Estimated void ratio distribution at KC-1

Figure 11 shows the estimated compression index distribution with depth at KC-1. The hollow circles represent the compression index from the oedometer tests in the soil investigations conducted in the vicinity of KC-1. The compression index varies within a range from approximately 0.6 to 1.8, with its distribution exhibiting a peak at a depth of around 25 meters (Yamamoto et al. 2010).

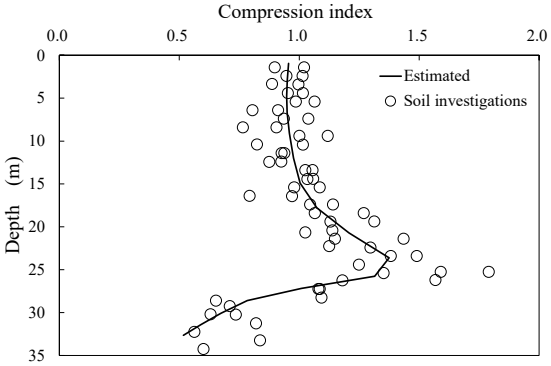

Figure 11. Estimated compression index distribution at KC-1

Figure 12 shows the estimated consolidation yield stress distribution with depth at KC-1. The hollow circles represent the consolidation yield stress from the oedometer tests in the soil investigations conducted in the

vicinity of KC-1. Figure 12 shows the effective overburden pressure derived from the void ratio and density of clay particles as a broken line. The consolidation yield pressure, which can be considered as the preconsolidation pressure, monotonically increases with depth. It slightly exceeded the overburden pressure, indicating that the Holocene clay was in an over-consolidated state despite the lack of a history of unloading.

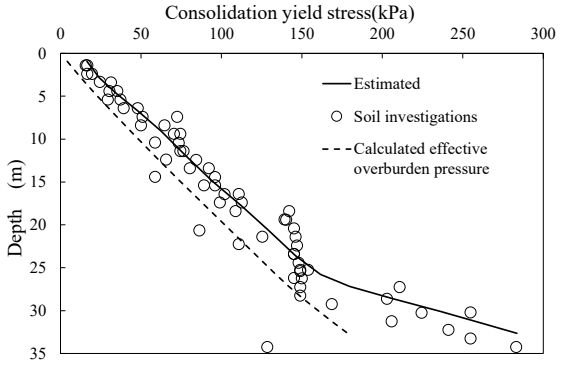

Figure 12. Estimated consolidation yield stress distribution at KC-1

Figure 13 shows the distribution of the estimated coefficient of permeability with depth at site KC-1. In this figure, the hollow circles represent the maximum coefficient of permeability obtained from the oedometer tests conducted during the soil investigation closest to the site. As shown in Fig. 14, the coefficient of permeability decreases with the void ratio; thus, the void ratio was incorporated as a crucial input in the process of estimating the permeability coefficient. The estimated coefficient of permeability is almost equal to the maximum value of the coefficient of permeability.

As shown in Figures 10–13, the estimation using artificial neural network can quantitatively reproduce the distribution of the compression index.

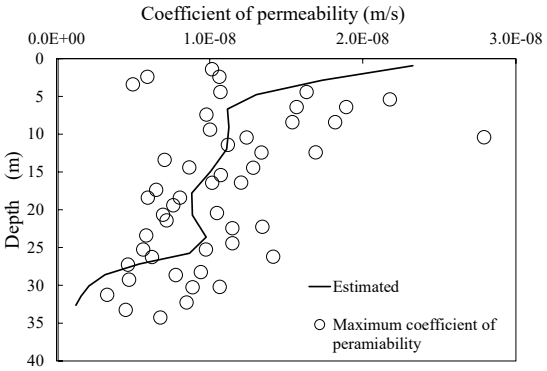

Figure 13. Estimated coefficient of permeability distribution at KC-1

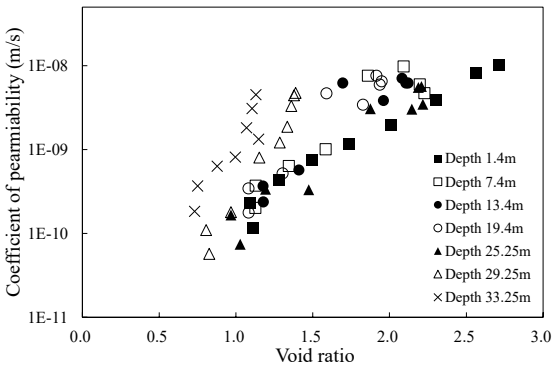

Figure 14. An example of relationship between void ratio and coefficient of permeability obtained from oedometer tests

6. Numerical simulation of settlement behavior using FEM

Figure 15 illustrates the analytical model. At the Kobe airport construction site, the sand drain method was employed specifically within the Holocene clay layer before the reclamation work to accelerate consolidation. An axisymmetric analytical model was used for analysis. Within this model, the drainage condition on most of the left side was simulated as a drained condition to accurately replicate the drainage effect of the sand drains. Furthermore, undrained conditions were maintained in the lower part because sand drains failed to fully penetrate the Holocene clay layer. Regarding the boundary conditions for the displacements, the horizontal displacements on both sides were fixed and both the horizontal and vertical displacements were constrained at the bottom of the analytical model.

The simplest constitutive equation was employed to simulate the consolidation behavior of Holocene clay, as follows:

$$e = e_0 - C_s \log\left(\frac{p_y}{p'_0}\right) - C_c \log\left(\frac{p'_0 + \Delta p}{p_y}\right) \tag{5}$$

where e_0 and p'_0 are the void ratio and effective overburden pressure in the initial state, respectively. C_c and C_s are the compression and swelling indices, respectively. In the analysis, it was assumed that C_s was one-twentieth that of C_c. p_y: consolidation yield pressure. Δp: reclamation load. Moreover, a soil-water coupled FEM was applied. The consolidation properties depicted in Figures 10–13 are used in the analysis.

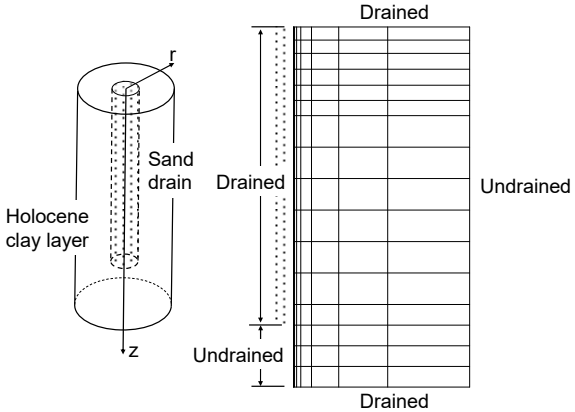

Figure 15. Analytical model

Figure 16 shows the reclamation history of KC-1. Reclamation started on 2000/8/20. The reclamation was nearly complete at the beginning of 2004. The average water depth is about 17m at the construction site. Therefore, the maximum reclamation load is almost 400kPa. (Hasegawa et al. 2007b)

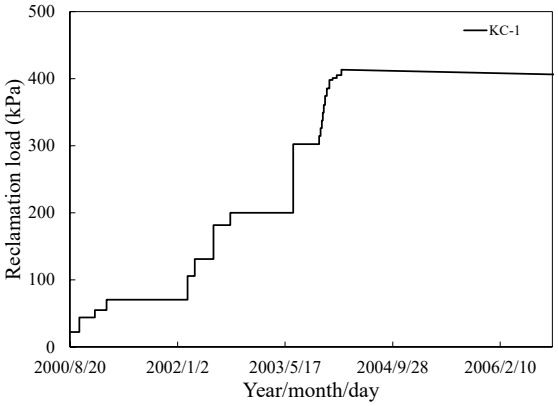

Figure 16. Reclamation history

Figure 17 shows a comparison between the measured and simulated settlements on the seabed surface. Measurements were taken to manage the reclamation work and maintain the runway. The numerical simulation closely matched the measured settlement from 2000/8/20 to the beginning of 2004. Beginning in 2004, the measured settlements progressively exceeded the simulated settlements. The differences between the measured and simulated settlements can be attributed to the consolidation settlement of the Pleistocene clay layers. In the case of man-made islands in Osaka Bay, such as Kansai International Airport, the consolidation settlement of Pleistocene clay layers became remarkable immediately after the completion of reclamation (Furudoi 2010). In this simulation, the focus was exclusively on analyzing the settlement behavior of the Holocene clay layer. Consequently, the consolidation properties of the Holocene clay layer can be appropriately estimated using artificial neural network techniques.

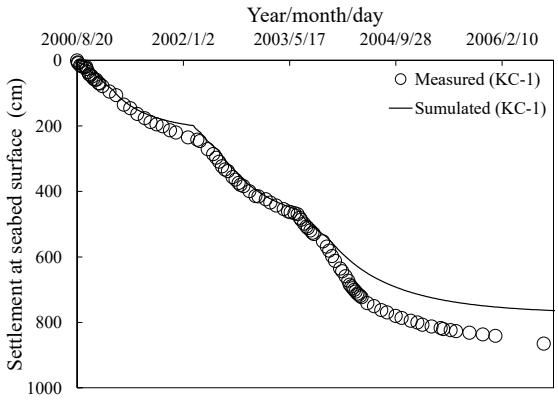

Figure 17. Comparison between the measured and simulated settlement at seabed surface

7. Conclusions

In this study, consolidation properties at arbitrary points within the Holocene clay layer at Kobe Airport were estimated using artificial neural network. Consolidation simulations were conducted using the estimated results to verify the validity of the estimated parameters. The main conclusions of this study are as follows:

1. The performance of an estimation model depends on the dataset used in the training phase. To avoid discrepancies in the estimation results across different models, it is advisable to build multiple estimation models using different datasets in the training phase and use the average of their estimates.
2. The method proposed by the authors enables the estimation of the consolidation properties of the Holocene clay layer at Kobe Airport.
3. Numerical simulations using the estimated consolidation properties can appropriately reproduce the settlement behavior owing to reclamation.
4. Artificial neural network allows the estimation of consolidation properties at arbitrary sites based on existing geotechnical investigations.

References

Furudoi, T. "The Second Phase Construction of Kansai International Airport Considering the Large and Long-Term Settlement of the Clay Deposits", Soils & Foundations, 50(6), pp. 805-816, 2010. https://doi.org/10.3208/sandf.50.805.

Hasegawa, N., Matsui, T., Tanaka, Y., Takahashi, Y., and Nambu, M. "Consolidation Properties of Holocene Layers below Seabed at Kobe Airport", Journal of the Japan Society of Civil Engineers C, 63(4), pp. 923-935, 2007a. (in Japanese), https://doi.org/10.2208/jscejc.63.923.

Hasegawa, N., Tanaka, Y., Takahashi, Y., Nambu, M., and Nonami, S. "Physical and Mechanical Properties of Reclaimed soil at Kobe Airport", Journal of the Japan Society of Civil Engineers C, 63(1), pp. 174-187, 2007b. (in Japanese), https://doi.org/10.2208/jscejc.63.174.

Mimura, M and Yamamoto, K. "Development of Geoinformatic Database and Its Utilization to Engineering Practice", Journal of Civil Engineering Research, 4(3A), pp. 1-13, 2014, https://doi.org/10.5923/c.jce.201402.01.

Oda, K., Yamamoto, S., and Kondoh, M. "Spatial Estimation of Unconfined Compression Strength of Osaka Plains via Deep Learning and Consideration of Its Estimation Accuracy", Proceedings of Geo-Risk 2023, Arlington County, Virginia, USA, 2023, pp. 191-199, https://doi.org/10.1061/9780784484975.

Yamamoto, T., Sakagami, T., Takahashi, Y., Yagiura, Y., Nambu, M., and Iizuka, A. "Establishment of Soil deformation analysis method at Kobe Airport", Journal of the Japan Society of Civil Engineers C, 66(3), pp. 457-471, 2010. (in Japanese), https://doi.org/10.2208/jscejc.66.457.